Electronic Supplementary Information

A wheel-like DNA nanosensor with background correction for analysis of miRNA-21 in living cells

Xiaoqing Li,[a] Fanghui Ma,[a] Lei Deng,[a] Minghui Yang,[a*] Xiang Chen[b,c*]

a *Hunan Provincial Key Laboratory of Micro & Nano Materials Interface Science, College of Chemistry and Chemical Engineering, Central South University, Changsha, Hunan Province 410083, China*

b *The Department of Dermatology, Xiangya Hospital, Central South University, Changsha 410008, China*

c *National Engineering Research Center of Personalized Diagnostic and Therapeutic Technology, Central South University, Changsha 410083, China*

1.EXPERIMENTAL SECTION

1.1 Apparatus and Materials.

Transmission electron microscope (TEM) characterization was performed on a FEI talos F200x G2 microscopy (USA). X-ray diffraction (XRD) results were obtained from an Empyrean spectrophotometer (Netherlands). The Fourier Transform Infrared Spectroscopy (FTIR) spectra was recorded on a Thermo IN10 FTIR spectrophotometer (USA). X-ray photoelectron spectroscopy (XPS) was recorded on a Thermo Scientific K-Alpha+ spectrometer (USA). The fluorescence measurements were measured on a F-7000 spectrofluorometer (Hitachi, Japan). The fluorescence imaging was performed on an inverted fluorescence microscope (IX 83, Olympus, Japan).

Ethylenediamine, neutral red (NR) and cetyltrimethyl ammonium bromide (CTAB) were obtained from Sigma-Aldrich. TRE Reagent was purchased from Sangon Biotech (Shanghai, China). Cell Counting Kit-8 (CCK8) was bought from Biosharp Life sciences. Human serum samples were acquired from the Xiangya hospital (Changsha, China). The DNA and RNA sequences used in this experiment were shown in Table S1. All other reagents were of analytical grade and no further purification was required. Deionized water was used throughout the experiment.

Table S1 DNA and miRNA sequences synthesized by Sangon Biotech (Shanghai, China)

Species	name	Sequence (5'-3')	dye
DNA	Harpin 1	AGC TGT AGT GTC CTC AGC TCC TCA ACA TCA GTC TGA TAA GCT AAC ACT ACA GAT AGG AGG AGG AGG A	5'-FAM
DNA	S 1	TCC TCC TCC TCC TCC TAT	5'-SH 3'-BHQ1
RNA	miR-21	UAGCUUAUCAGACUGAU GUUGA	
RNA	mis 1	UACCUUAUCAGACUGAU GUUGA	
RNA	Let-7a	UGAGGUAGUAGGUUGUA UAGUU	
RNA	miR-155	UUAAUGCUAAUCGUGAU AGGGGU	

1.2 Synthesis of red luminous carbon dots. The red emission carbon dots (CDs) were synthesized through a one-pot process.[1] In detail, 30 mg of NR was dissolved in 10 mL of deionized water under ultrasound. After completely dissolving, 150 μL of ethylenediamine was added and all of the solution was transferred into a Teflon-lined stainless-steel autoclave and continued heating for 5 hours at 200℃. The CDs product was finally obtained after centrifuging and dialyzing.

Prepare gold nanoparticles. Clean three-neck flask and condensing tube with aqua regia soak in advance. 100 mL of chloroauric acid (0.01%, w/w) was transferred into the flask and heated to boiling, newly prepared sodium citrate (2%, w/w) was added quickly and continued to heat for 10 minutes until the color of the solution changes from colorless to purplish red. Cool naturally to room temperature and store at 4℃.

1.3 Winding assembly of silica on the surface of CDs. The CDs were synthesized utilizing NR as precursor. For assembly of silica on CDs, in brief, CTAB (0.2 mmol) was added to 10 mL of synthesized CDs and sonicated for 20 min. Afterwards, 0.5 mL of $NH_3 \cdot H_2O$（25 wt.%）was added rapidly and 80 μL of tetraethyl orthosilicate (TEOS) was added dropwise with vigorous stirring. Then, the mixture was heated at 40℃ for 30 min.[2] After the reaction, the mixture was centrifuged and washed with deionized water until the supernatant was free of UV absorption. The yellow powder obtained after freeze-drying was CDs-SiO_2.

1.4 Assembly of gold nanoparticles and nucleic acid outside the CD_S-SiO_2 ring. A certain amount of CDs-SiO_2 was dissolved in deionized water with a concentration of 0.15 mg mL^{-1}. Then, 100 μL of (3-aminopropyl)triethoxysilane (APTES) was added to 5 mL of the solution and the mixture was shaken for 4 h to modify the amino group onto the surface of silica.[3] The Au NPs synthesized by sodium citrate reduction of chloroauric acid were mixed with the above solution at a ratio of 1:1 (v/v) and shaken overnight. The products were centrifuged and redispersed in deionized water. To continue the assembly of nucleic acid molecules on the surface of gold nanoparticles, the hairpin 1 strand (H1) was first heated at 95℃ for 5 min to open up the double-stranded DNA, and then the nucleic acid molecules were assembled according to the classical method of DNA assembly onto the surface of gold nanoparticles.[4] Briefly, 1 mL of CDs-SiO_2-Au NPs solution, 50 μL of H1 (5 μM) and 50 μL of S1 (5 μM) were added to a centrifuge tube and shaken slowly. After 16 h of reaction, an amount of NaCl solution was added to the centrifuge tube every 8 h until the final concentration of NaCl was 0.1 M. Finally, the excess nucleic acid molecules were removed by centrifugation at 12000 r/min for 20 min and the sediment, CDs-SiO_2-Au NPs-DNA (CSAD) were redispersed in the same

volume of deionized water for further use.

1.5 Ratio-dependent fluorescence detection of miR-21. In order to apply the prepared probe to realize miR-21 detection, 50 μL of CSAD, 100 μL of PBS buffer (pH=7.2-7.4, 0.01 M) and 50 μL of miR-21 standard solution of different concentrations were mixed and reacted at 37 ℃ for 1.5 h. The whole operation should be carried out under dark conditions. Fluorescence spectra were recorded after returning to room temperature.

1.6 Determination of miR-21 in human serum. To verify the practicality and reliability of the method, we measured and analyzed miR-21 in human serum. Two normal serum samples were diluted 100 times with RNase treated deionized water, and miR-21 was added into the serum with the concentration of 100 aM, 1 fM and 10 fM, respectively. The amount of miR-21 in the serum was then determined by the assay, and the recovery rates were calculated.

1.7 Cell culture and counting. MCF-7 and Hela cells were cultured in 1640 medium containing 10% fetal bovine serum and 1% double antibody (100 U mL^{-1} penicillin and 0.1 mg mL^{-1} streptomycin). After culture to logarithmic growth stage, the adherent cells were digested with trypsin containing EDTA to be suspended. A certain amount of medium was added to stop digestion, and the cell solution was centrifuged at 1000 r/min for 2 min. The supernatant was removed, and the cells were gently dispersed in the newly added medium. Finally, the cell concentration was calculated with the counting plate, and then diluted step by step to the concentration required for experiment.

1.8 Cell Cytotoxicity Study. In vitro cytotoxicity of the CSAD probe was evaluated using CCK8 assay in MCF-7 cells and Hela cells. In short, dilute the cell concentration to 5000 cells mL^{-1} and inoculate each well of 96 well plate with 100 μL cells. After cell adherence, the original medium solution was removed, and 100 μL of medium containing different concentrations of fluorescence probe (0.1 mg mL^{-1}, 0.2 mg mL^{-1}, 0.5 mg mL^{-1}, 1mg mL^{-1}, 2mg mL^{-1}) was added into each well, and a control experiment was performed with the addition of medium only. The solution in the wells was removed after 24 h and 1640 medium containing 10% CCK8 (v/v) was dropped into each well. The absorbances at 450 nm (OD450nm) and 630 nm (OD630nm) were determined two hours later. Cell viability was calculated by the following equation:

$$\text{Cell viability} = \frac{OD_{450nm/sample} - OD_{630nm/sample}}{OD_{450nm/control} - OD_{630nm/control}} \times 100\%$$

1.9 Quantitatively analyze miR-21 in MCF-7 and Hela cells. MCF-7 and Hela cells were cultured to

logarithmic growth stage and diluted to 10, 50, 100, 500, 1000, 5000 and 10000 (cells mL^{-1}) respectively, TRE reagent was used to extract intracellular total RNA according to the instructions. The specific process was as follows: TRE reagent (1 mL TRE/10cm^2 cells) was added to cells with different concentrations, and then deionized water without RNase was added to TRE lysis solution (2:5, v/v). After incubation at room temperature for 5 min, the lysate was centrifuged at 12000 rpm for 20 min. The upper solution containing RNA was transferred to an RNase-free centrifuge tube, isopropyl alcohol was added in equal volume and allowed to remain at room temperature for 20 min. The extracted RNA solution was centrifuged again at 12000 rpm for 15 min. The supernatant was removed and alcohol (75%, v/v) was added to wash the precipitation. After centrifugation again, the supernatant was removed and dried at room temperature for another 5 min. Afterwards, 50 μL of RNase-free deionized water was added to completely dissolve the RNA and RNA solution was stored at -80°C for later use.

1.10 Fluorescence imaging of miR-21 in MCF-7 and Hela cells. The logarithmic growing cells were cultured and counted, then diluted to different concentrations, and incubated with CSAD fluorescent probe for 2 hours. Then the cell imaging was observed under fluorescence inverted microscope.

2. **Characterization**

To confirm the step-by-step synthesis of the probe, several characterization strategies were applied. As demonstrated in Figure S1 A and B, TEM images show the morphologies of CDs and Au NPs, which are uniformly dispersed with particle sizes of about 1.57 nm and 13.51 nm, respectively. TEM images of CSAD show a circular spherical shape with a particle size of about 55 nm (Figure S1 C). HRTEM images show that the lattice spacing between adjacent fringes within the ring corresponds to the (108) crystal plane, which is consistent with the graphite carbon of CDs (Figure S1 D).[1, 5] The adjacent fringes on the ring correspond to the (111) crystal plane, which matches the SiO_2 crystal plane.[6, 7] In addition, there are additional lattice fringe spacing on the ring that corresponds to the (100) plane, which conforms to the crystal plane of Au NPs.[8] The above characterization results preliminarily verified the successful synthesis of CSAD.

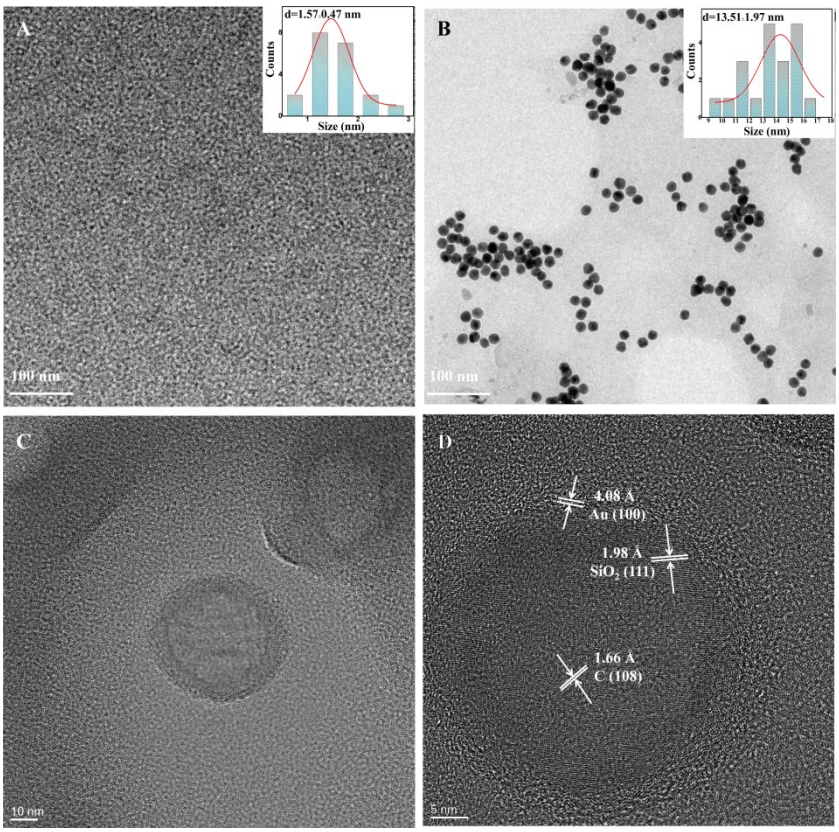

Figure S1. TEM images of CDs (A), Au NPs (B) and CSAD nanoprobe (C), and HRTEM image of CSAD nanoprobe (D). Insets: the size distributions of CDs (A) and Au NPs (B).

To further demonstrate the crystal structure of CSAD, X-ray diffraction (XRD) analysis was performed. As shown in Figure S2 A, after Au NPs and nucleic acid are loaded onto the surface of CDs, a similar XRD spectrum was observed when compared to CDs/SiO_2. The peak at 2θ=28.3º is attributed to (112) plane, which is consistent with the crystal shape of SiO_2.[6] The reflection in 2θ of 42.4º corresponds to (102) plane, which is consistent with the amorphous carbon of CDs.[5] No obvious diffraction peak of Au NPs was observed, which may be due to the limited loading amount of Au NPs. Fourier infrared spectroscopy (FTIR) and X-ray photoelectron spectroscopy (XPS) were used to study the changes of functional group and element composition during the synthesis of CSAD. The infrared spectra of CDs, CDs/SiO_2/Au and CSAD are shown in curves a-c in Figure S2 (B). The surface of CDs contains O-H and N-H (3380-3620 cm^{-1}), C-H (2890-2981 cm^{-1}), C=O (1642 cm^{-1}), C-N= (1402 cm^{-1}) and C-O (1060-1188 cm^{-1}) bond, in agreement with the literature results, which proves the successful preparation of CDs.[1] In addition, the surface functional groups of CDs do not change after winding silica, which proves that silica grows around it without changing surface properties of CDs. Moreover, the gradual assembly of Au NPs did not change the

characteristic peak of CDs as well, proving that the properties of CDs were retained during the preparation of CSAD.

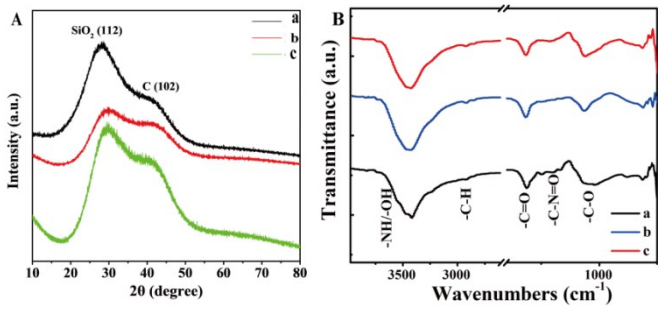

Figure S2. (A) XRD images of nanomaterials, in which a, b and c represent CDs/SiO_2, CDS/SiO_2/Au and CSAD, respectively. (B) FTIR spectra of (a) CDs, (b) CDs/SiO_2 and (c) CSAD.

The elemental composition of CSAD was further identified by XPS. The characteristic peaks of C1s, N 1s, O1s, Si 2p, Au 4f, S 2p and P 2p were observed in the wide scan XPS spectrum. Three peaks were observed in XPS spectra of C1s at about 285.3, 286.8 and 288.3 eV, corresponding to C-N, C-O and O-C-O bonds, respectively. In addition, three peaks were observed in the O 1s scanning spectrum, located at 530.9, 532.1 and 535.7 eV, respectively.[9] The first two peaks are associated with the oxygen in C-O and C-OH bonds, respectively, while the last peak is attributed to the Si-O bond, which is different from the CDs.[10] It was once again demonstrated that the silica winding process did not oxidize CD and successfully encircled CD (Figure S3 A and B) . For the synthesis process of CSAD, dynamic light scattering (DLS) was also used to test the surface potentials of the nanomaterials in different steps. As shown in Figure S3C, CDs/SiO_2 showed a strong positive potential due to the modification of -NH_2 onto the surface. After modifying gold nanoparticles, the charge was close to zero potential due to electrostatic binding. The next integration of H1 and S1 further shifted the charge to the negative potential, which also proved the successful completion of the stepwise modification process. Based on the above characterization results, it can be seen that CSAD was successfully synthesized as expected.

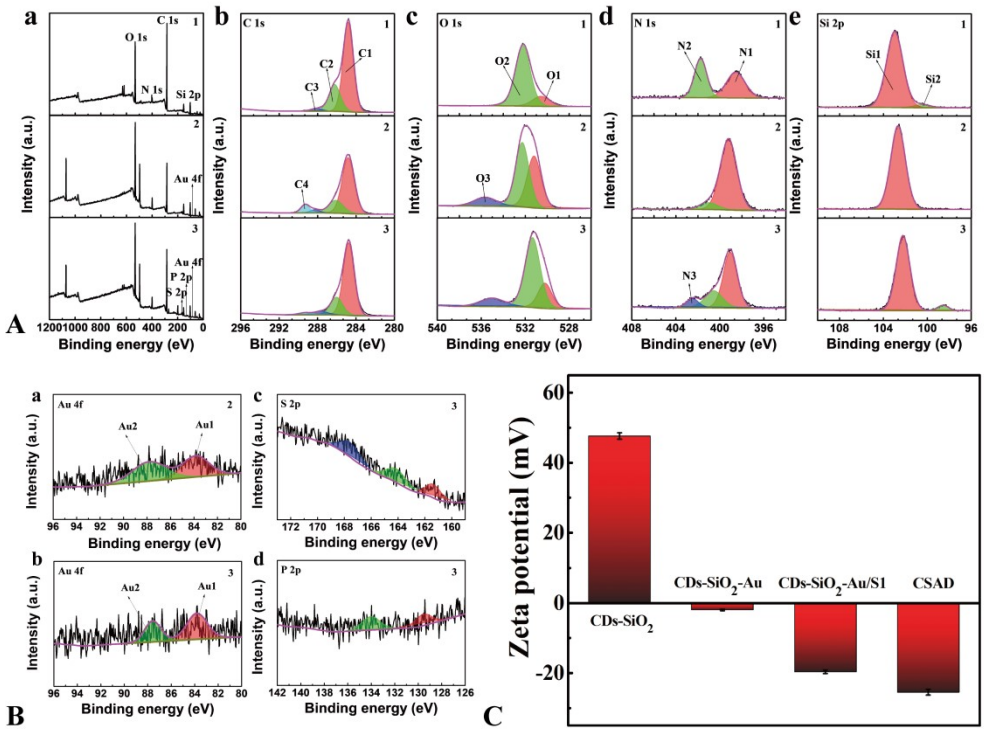

Figure S3. (A) X-ray photoelectron spectroscopy of (a) CDs/SiO_2 (1), CDs/SiO_2/Au NPs (2) and CSAD (3), (b) C 1s, (c) O 1s, (d) N 1s, (e) Si 2p in (1) CDs/SiO_2 (2) CDs/SiO_2/Au NPs and (3) CSAD. (B) XPS of (a) Au 4f in (2) CDs/SiO_2/Au NPs and (b) Au 4f, (c) S 2p, (d) P 2p in (3) CSAD. (C) Changes of surface potential during CSAD preparation.

3. Luminescence properties

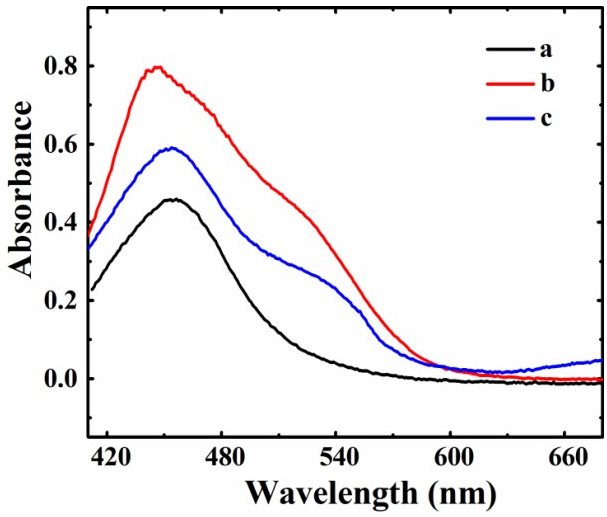

Figure S4. UV-vis spectra of (a) CDs, (b) CDs/SiO_2/Au NPs and (c) CSAD.

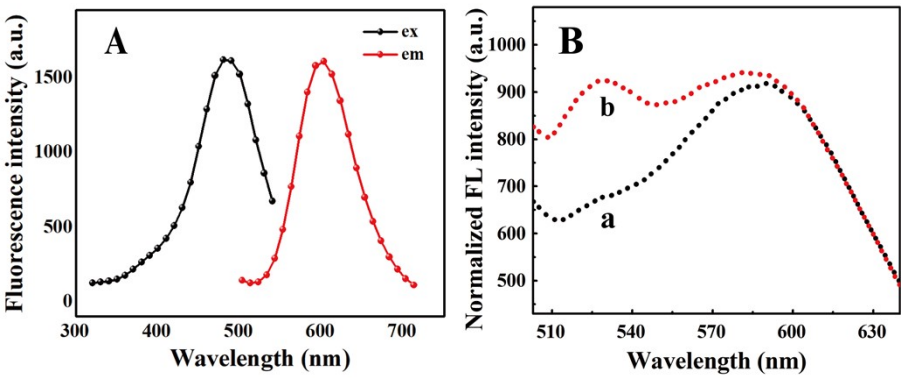

Figure S5. (A) Excitation and emission spectra of CDs; (B) Normalized fluorescence emission spectrum of CSAD (curve a) before and (curve b) after reaction with 100 pM miR-21. (ex=488 nm)

4. **Optimization of experimental conditions.** In order to optimize the influence of Au NPs particle size on the CSAD probe towards miR-21 analysis, Au NPs with particle sizes of 13 nm, 35 nm and 50 nm were prepared by using sodium citrate solutions with different mass fractions. To optimize the concentrations of H1 and S1, the probes were prepared by mixing with 50 μL of H1 (1 μM, 5 μM) and 50 μL of S1(1 μM, 5 μM). In order to optimize the reaction conditions between the probe and miR-21, different reaction temperatures (25, 37, 50℃) and reaction times (1, 1.5, 2, 2.5, 3 h) were adjusted. The fluorescence emission spectra of the probe after reaction with 100 pM of miR-21 were recorded under various conditions, and the emission intensity ratios at 598 nm and 527 nm were calculated. As shown in Figure S6, the optimal reaction conditions were as follows: 13 nm Au NPs, 50 μL 5 μM H1 and 50 μL 5 μM S1 were assembled into fluorescent probes and reacted with miR-21 at 37 ℃ for 1.5 h.

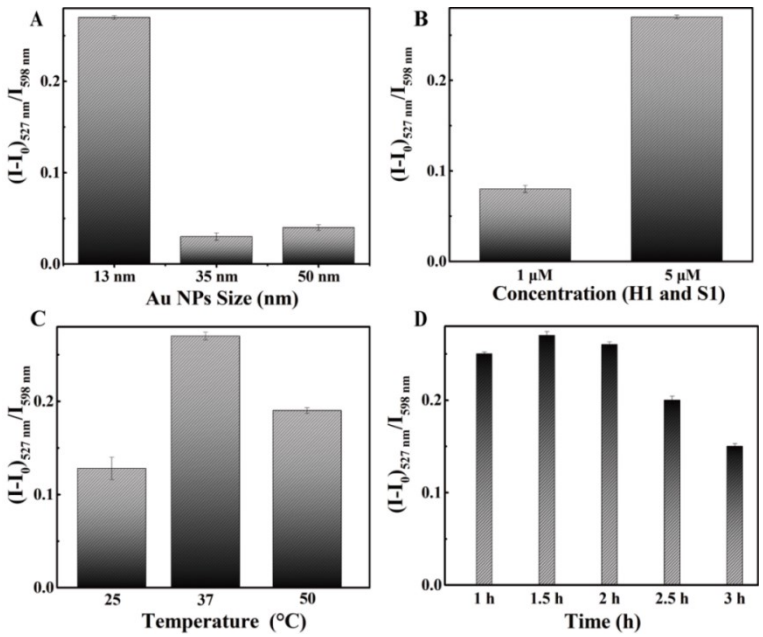

Figure S6. Optimization of experimental conditions (A) Size of Au NPs particle, (B) Concentration of H1 and S1, (C) Reaction temperature for CSAD and miR-21; (D) Reaction time of CSAD and miR-21. (n=3)

5.

Table S2. Comparison for the designed method and other optical assays

Composition of probe	Limit of detection	Linear range	Reference
Ag NPs	8.3 fM	0.01−50 pM	11
Carbon Dots	3 fM	10 - 500 fM	12
GO	0.02 nM	0.02-5 nM	13
FS	3.39 pM	0.01-1 pM	14
2D antimonene	10 aM	10 aM-10 pM	15
Palindromic DNA probe	25 pM	25 pM-250 nM	16
L-Au NPs@ZnO	18.6 aM	100 aM-100 pM	17
CSAD	2.5 aM	10 aM-100 pM	This work

6. **Recovery results of this assay for miR-21 detection in spiked human serum.** In order to verify the fluorescence nanosensing platform reported in this work may be applied to clinical assays, two normal human serum solutions were diluted 100 times with RNase-free water to simulate a clinical environment. Different concentrations of miR-21 (100 aM, 10 fM and 100 fM) were added to the diluted serum solution, and the serum miR-21 concentration was then measured. It can be seen in Table 1 that the recoveries of miR-21 in human serum samples range from 96.05% to 104.00% with the relative standard deviations of 0.43-3.96%, which can satisfy the quantitative analysis of miR-21 in real samples. These results indicate that the method is capable of sensitive determination of

miR-21 in real samples.

Table S3 Recovery results of this assay for miR-21 detection in spiked human serum (n=3)

Sample	added （fM）	found （fM）	RSD（%）	Recovery （%）
1	0.10	0.104	3.96	104.00
	10	9.723	2.89	97.23
	100	101.533	0.59	101.53
2	0.10	0.103	0.43	103.00
	10	9.605	1.82	96.05
	100	98.648	1.05	98.65

7. **Specific detection for miR-21.** To study the specificity of the sensor, several different miRNAs and their mixed solutions at 100 pM were detected by the sensor. As shown in Figure S7, the built-in background correction function ensures the sensor's specific detection to miR-21. Even if several miRNAs are mixed together for detection, the sensor still only has a significant response to miR-21.

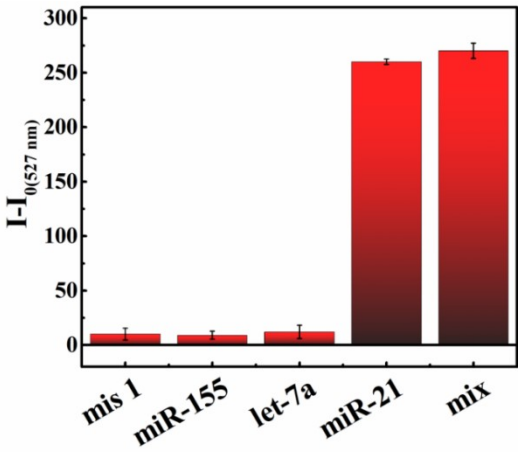

Figure S7. Selectivity of sensors for detection of 100 pM of miR-21 and other miRNAs.

8. Toxicity analysis of CSAD probe on MCF-7 and Hela cells. To test the toxicity of the CSAD probe to cells, MCF-7 and Hela cells were cultured with medium containing various concentrations of CSAD for 24 h. CCK8 was then added to the cells before optical density (OD) measurement. As shown in the Figure S8, after 24 hours of toxicity test, for both cells, only the concentration of 2mg mL^{-1} led to about 10% cell death, while other concentrations had almost no effect on cell viability. That is, the prepared nanoprobes had rather low toxicity to cells.

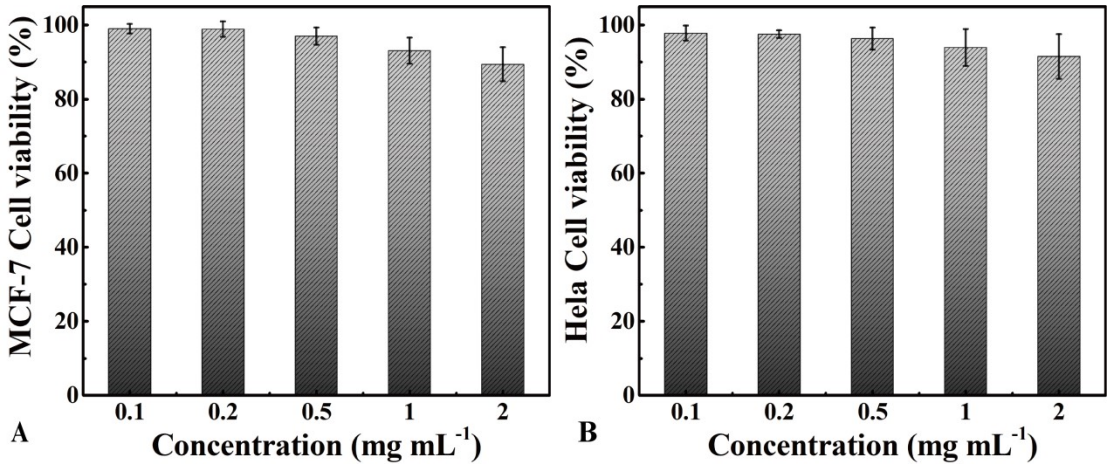

Figure S8. Cell viability of (A) MCF-7 cells and (B) Hela cells after cultured in different concentrations of nanoprobes for 24 h.(n=3)

9.

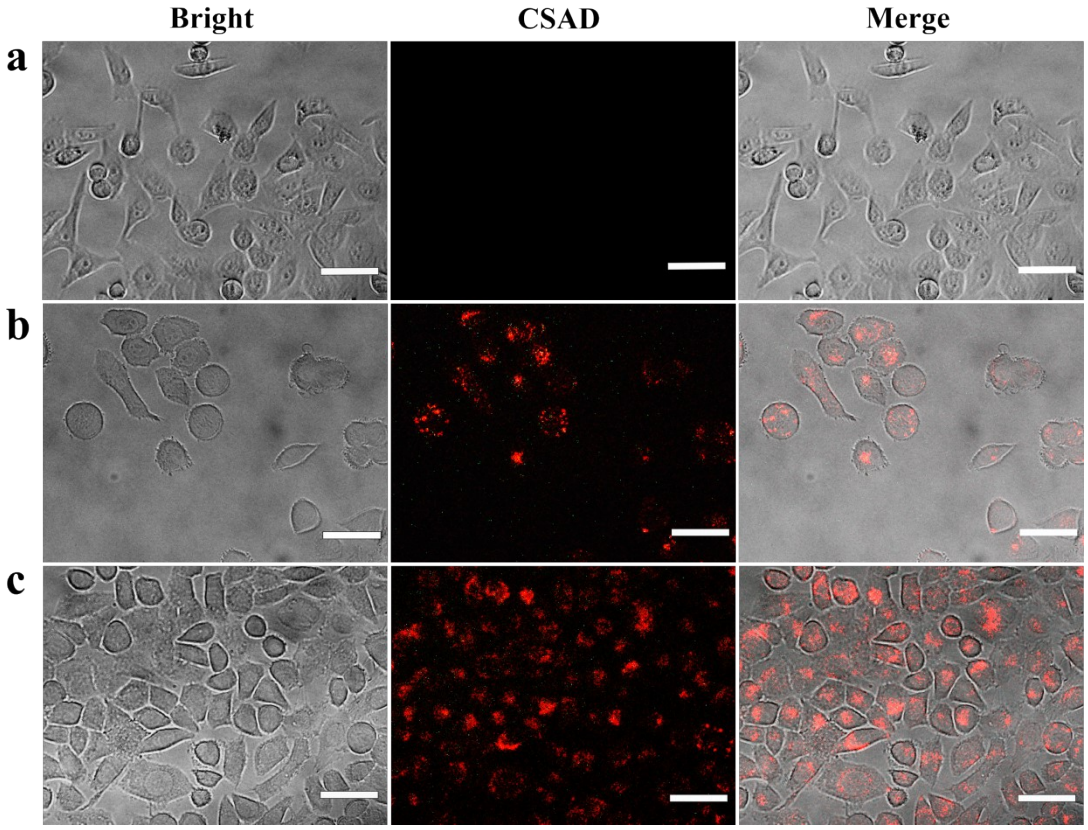

Figure S9. Inverted fluorescence microscopy images of MCF-7 cells treated without (a: 5000 cells mL^{-1}) and with CSAD (b: 5000 cells mL^{-1}) (c:10000s cell mL^{-1}) . Scale bar is 50 μm.

Reference

1 Y. Meng, Y. Jiao, Y. Zhang, H. Zhang, X. Gong, Y. Liu, S. Shuang and C. Dong, *Spectrochim. Acta. A.*, 2021, **251**, 119432.

2 T. Zhao, X. Zhang, R. Lin, L. Chen, C. Sun, Q. Chen, C.-T. Hung, Q. Zhou, K. Lan, W. Wang, Z. He, F. Zhang, A. A. Al-Khalaf, W. N. Hozzein, X. Li and D. Zhao, *J. Am. Chem. Soc.*, 2020, **142**, 20359-20367.

3 Q. Lyu, Q. Zhai, J. Dyson, S. Gong, Y. Zhao, Y. Ling, R. Chandrasekaran, D. Dong and W. Cheng, *Anal. Chem.*, 2019, **91**, 13521-13527.

4 X. Li, C. Shen, M. Yang and A. Rasooly, *Anal. Chem.*, 2018, **90**, 4764-4769.

5 S. A. Mathew, S. Dhanavel, Y. S. Hubert, V. Narayanan and A. Stephen, *J. Indian. Chem. Soc.*, 2019, **96**, 180-181.

6 S. E. Mousavi, H. Younesi, N. Bahramifar, P. Tamunaidu and H. Karimi-Maleh, *Chemosphere*, 2022, **297**, 133992.

7 S. K. Kazi, S. N. Inamdar, D. P. Kamble, K. S. Lohar, A. W. Suryawanshi and R. M. Tigote, *J. Chin. Chem. Soc-Taip.*, 2022, DOI: 10.1002/jccs.202200010, 1-10.

8 J. S. Jirkovsky, I. Panas, E. Ahlberg, M. Halasa, S. Romani and D. J. Schiffrin, *J. Am. Chem. Soc.*, 2011, **133**, 19432-19441.

9 Y. Zhong, X. Qiu, J. Gao and Z. Guo, *Isij. Int.*, 2019, **59**, 1098-1104.

10 K. Daware, M. Kasture, R. Kalubarme, R. Shinde, K. Patil, N. Suzuki, C. Terashima, S. Gosavi and A. Fujishim, *Chem. Phys. Lett.*, 2019, **732**, 136635.

11 G.-m. Ma, L.-w. Huo, Y.-x. Tong, Y.-c. Wang, C.-p. Li and H.-x. Jia, *Microchim. Acta.*, 2021, **188**, 355.

12 Y. Xia, L. Wang, J. Li, X. Chen, J. Lan, A. Yan, Y. Lei, S. Yang, H. Yang and J. Chen, *Anal. Chem.*, 2018, **90**, 8969-8976.

13 X. Ai, H. Zhao, T. Hu, Y. Yan, H. He and C. Ma, *Anal. Methods-UK*, 2021, **13**, 2107-2113.

14 W. Peng, Q. Zhao, M. Chen, J. Piao, W. Gao, X. Gong and J. Chang, *Theranostics*, 2019, **9**, 279-289.

15 T. Xue, W. Liang, Y. Li, Y. Sun, Y. Xiang, Y. Zhang, Z. Dai, Y. Duo, L. Wu, K. Qi, B. N. Shiyananju, L. Zhang, X. Cui, H. Zhang and Q. Bao, *Nat. Commun.*, 2019, **10**.

16 H. Xu, H. Niu, J. Liu, Y. Zhang, H. Yin, D. Liu, Z. Jiang, S. Yu and Z.-S. Wu, *Talanta*, 2020, **219**.

17 X. Zhang, W. Li, Y. Zhou, Y. Chai and R. Yuan, *Biosens. Bioelectron.*, 2019, **135**, 8-13.